Void Swelling as a Stochastic, Evolutionary Process

M. P. Surh, W. G. Wolfer

May 1, 2001

U.S. Department of Energy

Lawrence
Livermore
National
Laboratory

DISCLAIMER

This report has been reproduced directly from the best available copy.

Available electronically at http://www.doc.gov/bridge

Available for a processing fee to U.S. Department of Energy
And its contractors in paper from
U.S. Department of Energy
Office of Scientific and Technical Information
P.O. Box 62
Oak Ridge, TN 37831-0062
Telephone: (865) 576-8401
Facsimile: (865) 576-5728
E-mail: reports@adonis.osti.gov

Available for the sale to the public from
U.S. Department of Commerce
National Technical Information Service
5285 Port Royal Road
Springfield, VA 22161
Telephone: (800) 553-6847
Facsimile: (703) 605-6900
E-mail: orders@ntis.fedworld.gov
Online ordering: http://www.ntis.gov/ordering.htm

OR

Lawrence Livermore National Laboratory
Technical Information Department's Digital Library
http://www.llnl.gov/tid/Library.html

Void Swelling as a Stochastic, Evolutionary Process

Michael P. Surh and W. G. Wolfer

Lawrence Livermore National Laboratory, Mail Stop L-353, P.O. Box 808, Livermore, California 94551

Past theories of radiation swelling have mostly dealt with the effect of void growth on the steady-state rather than of void nucleation on the incubation of swelling. However, new analysis indicates that incubation and its dependence on dose rate, impurity concentrations, and temperature dramatically influences the cumulative experimental swelling. We present rate theory calculations of this void nucleation and growth that include the time-dependent coupling and evolution of point defect concentrations, void size distribution, and dislocation density. A transient, swelling-free period originates in the exponential sensitivity of nucleation to the temperature and point defect supersaturations and the dependence of the defect concentrations on the dose rate, temperature, and aggregate sink strengths. Specifically, simulations representing cold worked pure metals show delayed swelling that is governed by dislocation evolution towards a reduced, steady-state density. Impurity atoms are expected to affect the incubation period through the initial dislocation density and subsequent rate of evolution. We conclude that appreciable void swelling requires a sufficiently low concentration of network dislocation and dislocation loop sinks, and that incubation is the time required to achieve this state.

1. Introduction

Reactor materials can remain dimensionally stable during periods of irradiation up to the order of 10 dpa of total fluence. However, with continued irradiation, the material eventually begins to swell volumetrically, and it subsequently achieves a steady-state wherein its linear dimensions grow at a constant rate. That initial, swelling-free, "incubation stage" is a characteristic feature of radiation swelling in most reactor materials. Recent analysis suggests that the influence of this incubation period has not been fully accounted for when evaluating steady-state swelling behavior (1, 2, 3). Since incubation depends on radiation dose rates, temperature, impurity concentration, dislocation density, and other materials properties and steady-state often does not, this may confound the search for a microscopic understanding of swelling.

Swelling is widely considered to derive from the production of separate vacancies and interstitials from the residue of irradiation damage cascades (4, 5, 6, 7). During and after the damage cascade, the point defects can, variously, annihilate each other, aggregate in small voids or loops, form stacking fault tetrahedra, or be incorporated at pre-existing sinks like voids and dislocations (8). Analysis of the point defect interaction with these sinks indicates a biased flux that leads to void growth, dislocation climb, and a net swelling of the material (9). Absent the stable voids, the vacancies and interstitials should annihilate at the dislocations in equal numbers, so that there is no net climb and no net volume changes. Thus, incubation can be tentatively assigned to a delay in void nucleation and growth.

In this paper, we apply stochastic rate theory calculations to early-time void nucleation and growth. A mean-field treatment of stress and defect diffusion is used to derive parameters for evolution of the void size distribution within a Fokker-Planck formalism (6, 10). This approach has the advantage of treating both nucleation and growth processes on an equal footing. Here, we extend earlier such calculations to higher total fluences and longer times and incorporate a simplified treatment of the simultaneous evolution of dislocation density. As expected from classical nucleation theory, we find that nucleation rates are exponential in the vacancy chemical

potential. In turn, the nonequilibrium vacancy concentration is itself very sensitive to the total density of the sinks. That aggregate sink strength is initially dominated by dislocations, so no appreciable void nucleation occurs unless the dislocation concentration is low. We suggest that the incubation period is simply the time required to evolve the microstructure to a sufficiently low dislocation density that void nucleation becomes relevant. Factors which influence the initial dislocation density or the dislocation mobility and rate of evolution will affect the duration of the incubation period.

2. Theoretical Method

The microscopic process of vacancy aggregation and void nucleation and growth under nonequilibrium irradiation involves random aggregation or absorption of mobile point defects plus the emission of vacancies. This can be described by the theory of stochastic processes (11); for example, evolution of the ensemble void population can be studied from a master equation for the distribution of void sizes. However, a computational treatment of the full distribution of discrete sizes has been difficult, as voids range in size from a few to more than 10^5 lattice sites. For large voids, at least, it is possible to replace the atomic description with a continuum model to a good approximation. In that case, the population of discrete-size voids is replaced with a continuous size distribution, $P(x)$, evolving under a Fokker-Planck differential equation:

$$\frac{\partial P(x)}{\partial t} = -\frac{\partial}{\partial x}\left[K(x,t) - \frac{1}{2}\frac{\partial}{\partial x}Q(x,t)\right]P(x) + s(x) \quad (1)$$

for void radius, x. The evolution equation is characterized by a source term s, and nonlinear and time-dependent drift and diffusion parameters, K, and Q, obtained from the void-size transition rates of the master equation (10, 12). These parameters govern drift and diffusion of voids in their size space; they do not correspond to thermal diffusion of defects in the three-dimensional material.

Numerical solutions to such second order nonlinear evolution equations can be obtained an integral equation formal-

ism (10, 13), in a path integral scheme. In this approach, an approximate, short-time Green function is constructed for the Fokker-Planck differential equation, and the distribution is evolved in time by repeated application of this propagator. The method is numerically stable even for large time steps.

In practice, the void size distribution is re-discretized, and elements of the propagator matrix are calculated by double integration of the propagator over initial and final grid intervals (14, 13)

$$A_{ij}(\tau) = \frac{1}{\Delta x_i} \int dx_i \int dx_j G(x_i, x_j; \tau) \qquad (2)$$

with the approximate, Gaussian propagator:

$$G(x_i, x_j; \tau) = \frac{1}{\sqrt{2\pi Q(x_j)\tau}} exp\left[-(x_i - x_j - K(x_j)\tau)^2/(2Q(x_j)\tau)\right] \qquad (3)$$

In the original implementation, the first integration is efficiently computed from the numerical error function, while the second integration requires full, numerical quadrature. Much computational effort is expended to maintain accuracy in this quadrature, so we have substituted a Chebyshev polynomial interpolation. This can be integrated in closed form, and so the propagator matrix element is reduced to evaluation of a polynomial (15). Futhermore, after an initial period during which the void distribution and vacancy population may be rapidly evolving, we recompute the matrix at infrequent intervals.

We present calculations for fixed temperatures of 300K and a radiation flux of 10^{-6} dpa/s for a metal with dislocation densities range from 10^{12} to 10^{14} /m^2. Swelling appears quickly for the lower dislocation densities, and we find that numerical accuracy requires relatively small timesteps. The simulations are begun with timesteps of 10^{-5}s, which are logarithmically increased to a maximum of 2s during the first hour of simulated time. The numerical grid size, dx, is related to the timestep intervals τ, by $dx = \sqrt{Q(x,t)}\tau$ (10). This limits the bandedness of the diagonally-dominated propagator matrix to a manageable level. We truncate at up to 31 bands including the diagonal. In our experience, the conversion from discrete master equation to continuum and back to a discrete grid reduces the grid size by less than an order of magnitude. A coarser sampling would result in additional savings, but at the cost of reduced numerical accuracy.

The numerical convergence versus timestep appears to be controlled by the grid resolution at the small, unstable void sizes. Here, the density distribution may vary by orders of magnitude between voids with n and $n + 1$ vacancies, so the assumption of a continuous distribution function requires a fine gridding. It is precisely the random passage of small, unstable voids across the threshold that controls the nucleation rate, so the calculations are very sensitive to the treatment of this region.

3. Results and Analysis

We first study the artificial case of a fixed, time-independent dislocation density and examine trends in
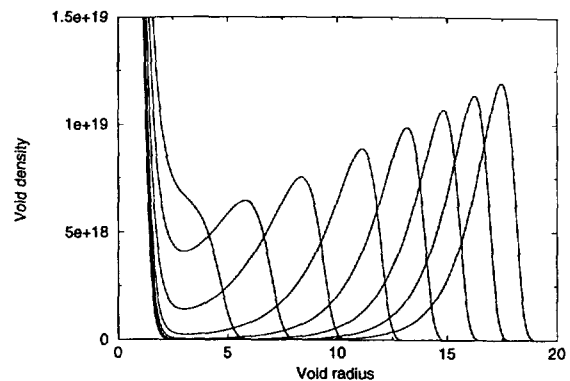
FIGURE 1. Void size distribution, P, versus radius, x (in units of burgers vector) at various time intervals after the onset of irradiation ($t = 4, 8, 14, 24, 34, 44, 54$, and 64 minutes). These results are for a time-independent, low density of dislocation sinks (2×10^{12} m^{-2}). The distribution function includes factors of x^2, so the density of voids with radii from x to $x + dx$ is: $d\rho \simeq P(x)dx$.

swelling. There are two qualitative limits that are of interest. The first occurs for relatively low dislocation densities or high radiation dose rates; the second is at high dislocation densities or very low dose rates. The limits are separated by their (high or low, respectively) vacancy supersaturation at initial times.

The first limit case gives a rapid aggregation and high concentration of vacancy dimers and larger aggregates.The initial growth of voids from the excess monomers is due to the diffusive component, Q, of the Fokker-Planck equation because the drift term, $K < 0$. Thus, at early times, the distribution is peaked at the vacancy monomer and broadens to larger sizes with increasing time (see Fig. 1, t = 4 min.). As the void distribution spreads beyond the threshold size for stable voids, there is a net drift towards larger sizes (since $K > 0$), and these stable voids grow steadily. The nucleation rate is given by the flux of voids through the threshhold and is related to the void density and diffusivity there (since $K = 0$ at the threshhold).

In these low dislocation density calculations, the void sink strength subsequently rises to become significant relative to the pre-existing dislocation sinks. As total sink strength increases with time, the vacancy concentration decreases (Fig. 2). The stable void size moves to larger sizes, the density of voids around the threshhold drops precipitously (Fig. 1), and the void nucleation essentially halts. The void size distribution now consists of a well-defined bulge that has pinched off from the unstable vacancy multimers at early times (Fig. 1, t $\simeq$ 30 minutes). Henceforth, that bulge steadily evolves towards larger sizes while the total area it encompasses (number of such voids overall) is constant. This void growth without appreciable further nucleation coincides with a steady-state, linear volume swelling versus time (see Fig. 2).

A second limit is obtained when the initial vacancy concentration is very low, at low dose rate or high dislocation sink density. In this case, the vacancy monomer osmotic pressure is small. The initial void distribution is peaked at the monomers, and only the exponential tail reaches to the stable void threshhold (Fig. 3, t = 1 hour). Subsequently,
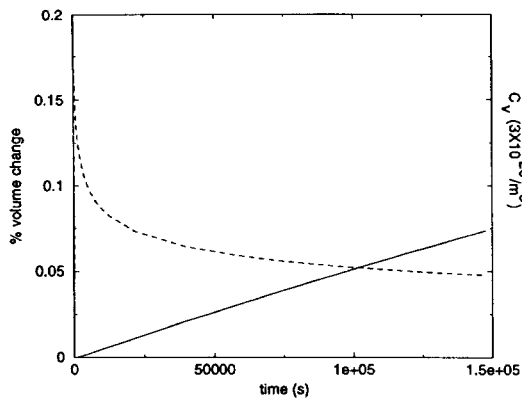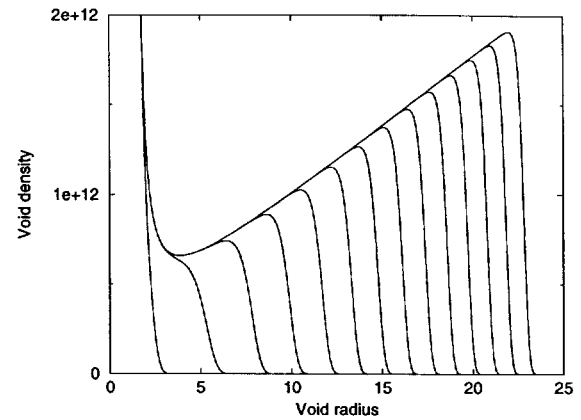
FIGURE 2. Percent of volume swelling and vacancy concentration versus time for dislocation density of 2×10^{13} m^{-2}. Percent volume change is shown with solid lines and labels on the left axis; vacancy concentrations are plotted as a dashed line and labeled on the right.

FIGURE 3. Density of voids versus radius (as in Fig. 1) for a high density of dislocation sinks (2×10^{14} m^{-2}) at times $t = 1 + 5(i - 1)$ hours (for $i = 1$ to 14).

FIGURE 4. Percent of volume swelling versus time for dislocation density of 2×10^{14} m^{-2}. The vacancy density is quasistatic at 6.7×10^{17} m^{-3}.

the accumulated void sink strength remains negligible compared to the dislocation sinks. Therefore, the Fokker-Planck model parameters, K and Q are quasi-stationary, and the nucleation rate for stable voids is constant in time. This incubation limit persists while the accumulated voids remain inconsequential compared to the aggregate sink strength. Important microstructural changes which involve the dislocation distribution are ignored in this simple model example.

The distribution of unstable and small, stable voids, quickly reaches a quasi-stationary limit (Fig. 3, t > 1 hour). Because of this, the steady flux of nucleating voids ultimately accumulates at the upper limit of the void size distribution. The leading edge, x_{max}, advances at a rate given by drift, $K(x_{max})$ (K is effectively independent of time, here), and so the height of the distribution at the growing edge, is controlled by the nucleation rate (i.e., $P(x_{max})K(x_{max}) \simeq J_{nuc}$). A characteristic, linear distribution results versus void radius with a total swelling rate, $d(ln(V))/dt \simeq t^3$ (Fig. 4).

Finally, we display the dependence of swelling rate on (time-independent) dislocation density between these two limits of behavior in Fig. 5. Again, temperature is 300 K and dose rates are 10^{-6} dpa/s. Both transient and steady-state behaviors can be seen. The swelling rates for the higher, but still reasonably achievable, dislocation densities are hardly visible on a linear plot when compared to the results for low dislocation density.

The increase in swelling versus dislocation density is so dramatic that even a gradual decrease in dislocation density versus time will cause an abrupt appearance of swelling. We show this with a simple model of time-dependent dislocation densities in Figs. 6 and 7. We choose a simple, exponentially decaying dislocation density from high to low sink strengths. The decay time (or decay dose) is chosen to be relatively small, so that the significant changes occur during simulation times of order 10^6 seconds. The results are encouraging for future work which will include the realistic evolution of dislocations.
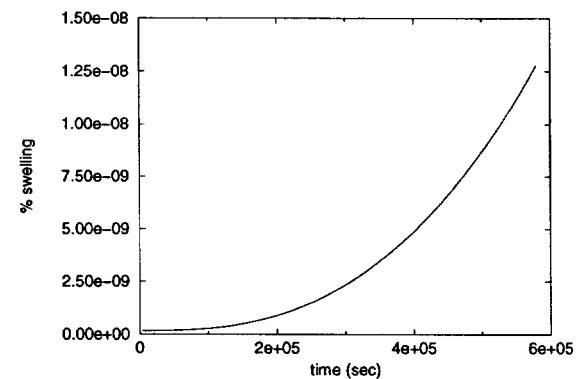
4. Conclusion and Future Work

Our simulated nucleation behavior is consistent with the incubation period observed in some cold-worked metals. Plausible dislocation densities reach levels such that no significant void nucleation occurs in our calculations. We anticipate that incorporation of more realistic models of dislocation evolution versus radiation dose (16) into our model will produce similar incubation periods to experiment. In summary, the initial stages of radiation damage transform the microstructure by dislocation climb and glide and annihilation. However, there is no net climb and no swelling until significant numbers of voids nucleate. Swelling occurs only after the stored dislocation density has annihilated sufficiently. Our proposed mechanism is also consistent with observations of a longer incubation time for impure metals (17). Solute atoms can segregate at the dislocations, limit their mobility, and delay their annihilation. Solute drag is also pertinent for small prismatic loops which develop from interstitial defects in radiation cascade simulations; there is a greater trapping effect for loops than for individual interstitials. If interstitial prismatic loops are immobilized and accumulate at a high density, they will efficiently annihilate vacancies and inhibit void
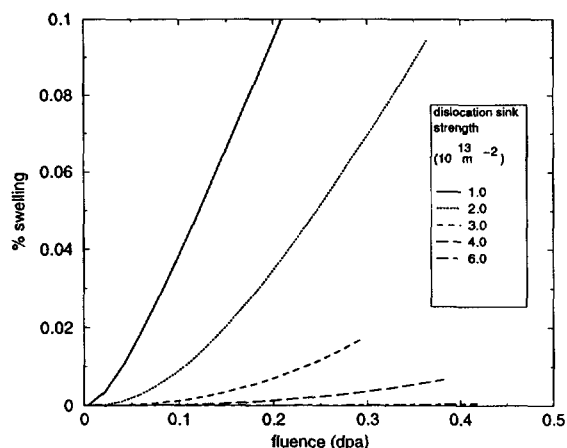
FIGURE 5. Fractional volume swelling versus time for dislocation densities of 1, 2, 3, 4, and 6 $\times 10^{13}$ m^{-2}.
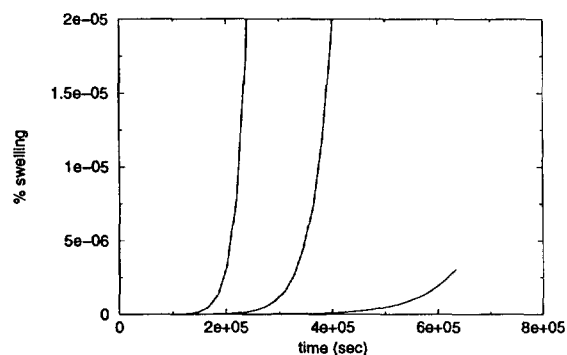
FIGURE 6. Percentage of volume swelling versus time for model time-dependent dislocation densities exponentially decaying from 2×10^{14} m^{-2} to 2×10^{13} m^{-2}. There are three curves displayed, with (rapid) exponential decay times of 10^5 s, 2×10^5 s, and 5×10^5 s. The different relaxation rates are meant to exhibit the influence of solute atoms on dislocation glide mobility and annihilation or coalescence rates under irradiation climb.
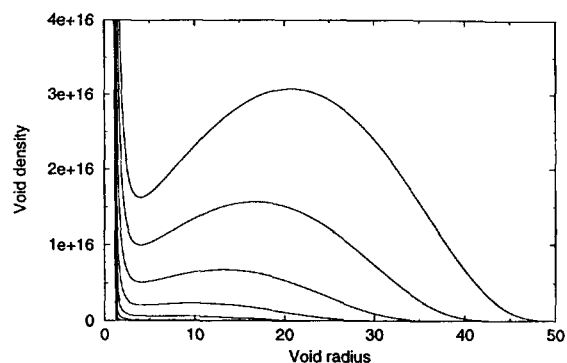

FIGURE 7. Void size distribution for the time dependent dislocation density calculation with 10^5 s dislocation decay time. Results are displayed for 10 hour intervals from 1 to 81 hours ($\simeq 3 \times 10^5$s), although only the later times are distinguishable on this scale.

nucleation. Reduction of the prismatic loop density by glide and coalescence must then await depletion of the solute atmosphere to precipitates.

References

1. F.A. Garner, J. Nucl. Mater. **122/123**, 459 (1984).
2. F.A. Garner, J. Nucl. Mater. **205**, 98 (1993).
3. F.A. Garner, C.A. Black, and D.J. Edwards, J. Nucl. Mater. **245**, 124 (1997).
4. A.D. Brailsford and R. Bullough, J. Nucl. Mater. **44**, 121 (1972).
5. A.S. Brailsford and R. Bullough, J. Nucl. Mater. **69/70**, 434 (1978).
6. W.G. Wolfer, J. Nucl. Mater. **122/123**, 367 (1984).
7. C.H. Woo, A.A. Semenov, and B.N. Singh, J. Nucl. Mater. **206**, 170 (1993).
8. M.J. Caturla, N. Soneda, E. Alonso, B.D. Wirth, T.D. de la Rubia, J.M. Perlado J. Nucl. Mater. **276** 13 (2000)
9. A.D. Brailsford and R. Bullough, Phil. Trans. Royal Soc. London **A302**, 87 (1981).
10. M.F. Wehner and W.G. Wolfer, Phil. Mag. A **52**, 189 (1985).
11. H. Risken, *The Fokker-Planck Equation: Methods of Solution and Applications*, 2nd ed. (Springer, New York, 1996).
12. These parameters, K and Q, govern drift and diffusion of voids in their size space; they do not correspond to thermal diffusion of defects in the three-dimensional material.
13. J.B. Adams and W.N.G. Hitchon, J. Comp. Phys. **76**, 159 (1988).
14. M.F. Wehner and W.G. Wolfer, Phys. Rev. A **27**, 2663 (1983).
15. W.H. Press, B.P. Flannery, S.A. Teukolsky, and W.T. Vetterling, *Numerical Recipes*, (Cambridge University Press, New York, 1990).
16. W.G. Wolfer and B.B. Glasgow, Acta Metall. **33**, 1997 (1985).
17. F.A. Garner and W.G. Wolfer, J. Nucl. Mater. **102**, 143 (1981).